

Electromagnetic Wave Propagation in Media with Indefinite Permittivity and Permeability Tensors

D. R. Smith and D. Schurig

(Dated: November 26, 2002)

We study the behavior of wave propagation in materials for which not all of the principle elements of the permeability and permittivity tensors have the same sign. We find that a wide variety of effects can be realized in such media, including negative refraction, near-field focusing and high impedance surface reflection. In particular a bi-layer of these materials can transfer a field distribution from one side to the other, including near-fields, without requiring internal exponentially growing waves.

The range of available electromagnetic material properties has been broadened by recent developments in structured media, notably Photonic Band Gap materials and metamaterials. These media have allowed the realization of solutions to Maxwell's equations not available in naturally occurring materials, fueling the discovery of new physical phenomena and the development of devices. Photonic crystals, for example, can modify the radiative density of states associated with nearby electromagnetic sources. Optical effects such as superradiance [1], enhanced or inhibited spontaneous emission [2], ultra-refraction [3] and even negative refraction [4, 5] have been predicted for various photonic lattice configurations.

Photonic crystal effects typically occur when the wavelength is on the same order or smaller than the lattice constant of the crystal. Metamaterials, on the other hand, have unit cell dimensions much smaller than the wavelength of interest. A homogenization process can thus be applied, allowing the otherwise complicated composite medium to be described conveniently by a permittivity tensor (ϵ) and a permeability tensor (μ) [6], rather than by band diagrams.

In 2000, it was shown experimentally that a metamaterial composed of periodically positioned scattering elements, all conductors, could be interpreted as having simultaneously a negative effective ϵ and a negative effective μ [7]. Such a medium had been previously shown by Veselago to be consistent with Maxwell's equations [8], but had never been demonstrated in a naturally occurring material or compound. A medium with simultaneously isotropic and negative ϵ and μ supports propagating solutions whose phase and group velocities are antiparallel; equivalently, such a material can be rigorously described as having a negative index of refraction [9]. An experimental observation of negative refraction was reported using a metamaterial composed of wires and split ring resonators deposited lithographically on circuit board material [10].

The prospect of negative refractive materials has generated considerable interest, as this simply stated material condition suggests the possibility of extraordinary wave propagation phenomena, including near-field focusing [11]. So remarkable have been the claims surrounding negative refraction, that some researchers have

been prompted to examine critically the achievability of negative refraction in existing metamaterials [12, 13]. While such concerns might appear relevant in the context of frequency-dispersive materials, the interpretation of these structured materials as negative refractive has been entirely consistent with all aspects of reported experimental data [7, 10], as well as with numerical simulations of both monochromatic and modulated beams [14, 15]. For the purposes of this Letter, we thus assume that the descriptions presented here will be applicable to real materials, although the extent to which this is true remains a topic of active pursuit.

Lindell et al. [16] have shown that the property of negative refraction is not confined to materials with negative definite ϵ and μ , but can be expected to occur in certain classes of uniaxially anisotropic media. In addition to exhibiting negative refraction, some classes of anisotropic media have very unusual dispersion relations, characterized for example by hyperbolic dispersion curves. The range of electromagnetic wave propagation behavior expected for such materials greatly extends beyond that available in isotropic negative refractive materials, and motivates our pursuit here to find configurations that take advantage of the unique properties.

To simplify the proceeding analysis, we assume a linear material with no magnetoelectric coupling, so that the media can be fully described by a permittivity, ϵ , and permeability, μ , tensor. [Bianisotropy effects have typically played a minor role in the overall response of the experimental metamaterials, and can be mitigated by design [17].] We further assume that these tensors are simultaneously diagonalizable, having the form

$$\epsilon = \begin{pmatrix} \epsilon_x & 0 & 0 \\ 0 & \epsilon_y & 0 \\ 0 & 0 & \epsilon_z \end{pmatrix} \quad \mu = \begin{pmatrix} \mu_x & 0 & 0 \\ 0 & \mu_y & 0 \\ 0 & 0 & \mu_z \end{pmatrix}. \quad (1)$$

Metamaterials can be readily constructed that closely approximate these ϵ and μ tensors, with elements of either algebraic sign. In fact, the scattering elements comprising the metamaterials used to demonstrate negative refraction [10] are appropriate building blocks for the classes of materials to be discussed here, (see Fig. 1.)

We are interested in an anisotropic medium in which not all of the principle components of the ϵ and μ ten-

sors have the same sign. For brevity, we refer to such a medium as *indefinite*. We will consider layered media with surfaces normal to one of the principle axes, which we define to be the z -axis. We demonstrate our analysis using a plane wave with the electric field polarized along the y -axis, though it is generally possible to construct media that are polarization independent, or exhibit different classes of behavior for different polarizations.

$$\mathbf{E} = \hat{\mathbf{y}}e^{i(k_x x + k_z z - \omega t)}. \quad (2)$$

Plane wave solutions to Maxwell's equations with this polarization have $k_y = 0$ and satisfy:

$$k_z^2 = \varepsilon_y \mu_x \frac{\omega^2}{c^2} - \frac{\mu_x}{\mu_z} k_x^2. \quad (3)$$

Since we have no x or y oriented boundaries or interfaces, real exponential solutions, which result in field divergence when unbounded, are not allowed in those directions. Thus k_x is restricted to be real. Also, since k_x represents a variation transverse to the surfaces of our layered media, it is conserved across the layers, and naturally parameterizes the solutions.

In the absence of losses, the sign of k_z^2 can be used to distinguish the nature of the plane wave solutions. $k_z^2 > 0$ corresponds to real valued k_z and propagating solutions. $k_z^2 < 0$ corresponds to imaginary k_z and exponentially growing or decaying (evanescent) solutions. When $\varepsilon_y \mu_z > 0$, there will be a value of k_x for which $k_z^2 = 0$. This value, which we denote k_c , is the cutoff wave vector separating propagating from evanescent solutions. From Eq. (3) this value is $k_c = \frac{\omega}{c} \sqrt{\varepsilon_y \mu_z}$. We identify four classes of media based on their cutoff properties:

	Media Conditions		Propagation
Cutoff	$\varepsilon_y \mu_x > 0$	$\mu_x / \mu_z > 0$	$k_x < k_c$
Anti-Cutoff	$\varepsilon_y \mu_x < 0$	$\mu_x / \mu_z < 0$	$k_x > k_c$
Never Cutoff	$\varepsilon_y \mu_x > 0$	$\mu_x / \mu_z < 0$	all real k_x
Always Cutoff	$\varepsilon_y \mu_x < 0$	$\mu_x / \mu_z > 0$	no real k_x

Note the analysis presented here is carried out at constant frequency, and that the term *cutoff* always refers to the transverse component of the wave vector, k_x , not the frequency, ω . Iso-frequency contours, $\omega(\mathbf{k}) = \text{const}$, show the required relationship between k_x and k_z for plane wave solutions (Fig. 2).

To understand wave refraction at an interface between vacuum and an indefinite medium, we must first examine the general relationship between the directions of energy and phase velocity for waves propagating within an indefinite medium. We can accomplish this by calculating the group velocity, $\mathbf{v}_g \equiv \nabla_{\mathbf{k}} \omega(\mathbf{k})$. \mathbf{v}_g specifies the direction of energy flow for the plane wave, and is not

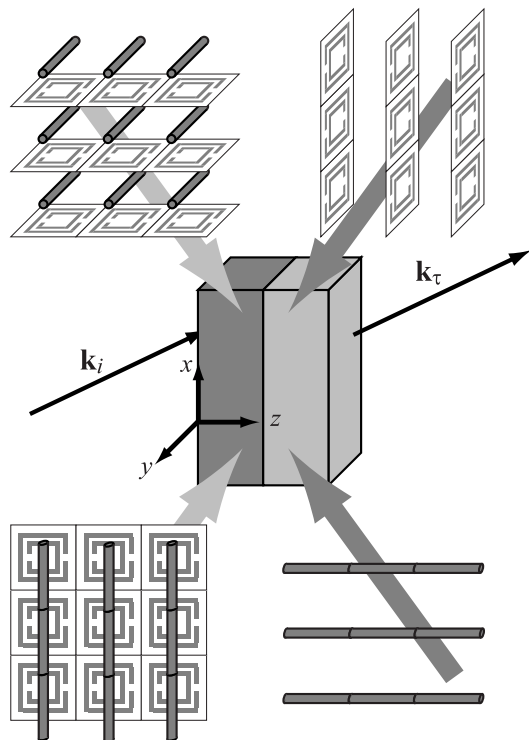


FIG. 1: A bilayer composed of indefinite media implemented using split ring resonators and straight wires. The structures in the top of the figure implement *never cutoff* media for electric y -polarization. Top left is negative refracting and top right is positive refracting. The structures in the bottom of the figure do the same for magnetic y -polarization.

necessarily parallel to the wave vector. $\nabla_{\mathbf{k}} \omega(\mathbf{k})$ must lie normal to the iso-frequency contour, $\omega(\mathbf{k}) = \text{constant}$, but may lie on either side, as illustrated in Fig. 2. To determine the correct direction, we utilize the dispersion relation in Eq. (3) to calculate $\nabla_{\mathbf{k}} \omega(\mathbf{k})$. Performing an implicit differentiation of Eq. (3) leads to a result for the gradient that does not require square root branch selection, removing any sign confusion. To obtain physically meaningful results, a causal, dispersive response function, $\xi(\omega)$, must be used to represent the negative components of ε and μ , since these components are necessarily dispersive [18]. The response function should assume the desired (negative) value at the operating frequency, and satisfy the causality requirement that, $\partial(\xi\omega)/\partial\omega \geq 1$ [9, 18]. Combing this with the derivative of Eq. (3) determines which of the two possible normal directions applies, without specifying a specific functional form for the response function. Fig. 2 relates the direction of the group velocity to a given material property tensor sign structure.

Having calculated the energy flow direction, we can determine the refraction behavior of indefinite media by applying two rules: (1) the transverse component of the wave vector, k_x , is conserved across the interface, and

(2) energy carried into the interface from free space must be carried away from the interface inside the media; i.e., the normal component of the group velocity, v_{gz} , must have the same sign on both sides of the interface. Fig. 2 shows typical refraction diagrams for the three types of media that support propagation.

Despite the interesting refraction properties associated with indefinite media, a finite slab of indefinite material will in general present a significant impedance mismatch to waves incident from vacuum. We can, however, increase the transparency at a given frequency by combining a layer of indefinite material with a second layer possessing the same dispersion and impedance but opposite refractive index. Such a compensated bilayer will have inter-layer relative impedance near unity, and will exhibit zero phase shift from one side to the other, for all plane wave components.

To illustrate the possibilities associated with compensated bilayers of indefinite media, we first recall that a motivating factor in the recent metamaterials effort has been the prospect of near-field focusing. Pendry showed theoretically that a planar slab with isotropic $\varepsilon = \mu = -1$, could act as a lens with resolution well beyond the diffraction limit. It is difficult, however, to realize significant sub-wavelength resolution with an isotropic negative index material, as the required exponential growth of the large k_x field components across the negative index lens leads to extremely large field ratios[19]. Sensitivity to material loss and other factors can significantly limit the sub-wavelength resolution.

By combining positive and negative refracting layers of *never cutoff* indefinite media, we can produce a compensated bilayer that accomplishes near-field focusing in a similar manner to the perfect lens, but with significant advantages. Fig. 2 indicates that for the same incident plane wave, the z -component of the transmitted wave vector is of opposite sign for these two materials. Combining appropriate lengths of these materials results in a composite indefinite medium with unit transfer function. We can see this quantitatively by considering the general expression for the transfer function of a bilayer.

$$T = 8 \begin{bmatrix} e^{i(\phi+\psi)} (1 - Z_0) (1 + Z_1) (1 - Z_2) + \\ e^{i(\phi-\psi)} (1 - Z_0) (1 - Z_1) (1 + Z_2) + \\ e^{i(-\phi+\psi)} (1 + Z_0) (1 - Z_1) (1 - Z_2) + \\ e^{i(-\phi-\psi)} (1 + Z_0) (1 + Z_1) (1 + Z_2) \end{bmatrix}^{-1} \quad (4)$$

The relative effective impedances are defined as

$$Z_0 = \frac{q_{z1}}{\mu_{x1} k_z}, \quad Z_1 = \frac{\mu_{x1} q_{z2}}{\mu_{x2} q_{z1}}, \quad Z_2 = \mu_{x2} \frac{k_z}{q_{z2}}. \quad (5)$$

where \mathbf{k} , \mathbf{q}_1 and \mathbf{q}_2 are the wave vectors in vacuum and the first and second layers of the bilayer respectively. The individual layer phase advance angles are defined as $\phi \equiv q_{z1} L_1$ and $\psi \equiv q_{z2} L_2$, where L_1 is the thickness of the first layer and L_2 is the thickness of the second

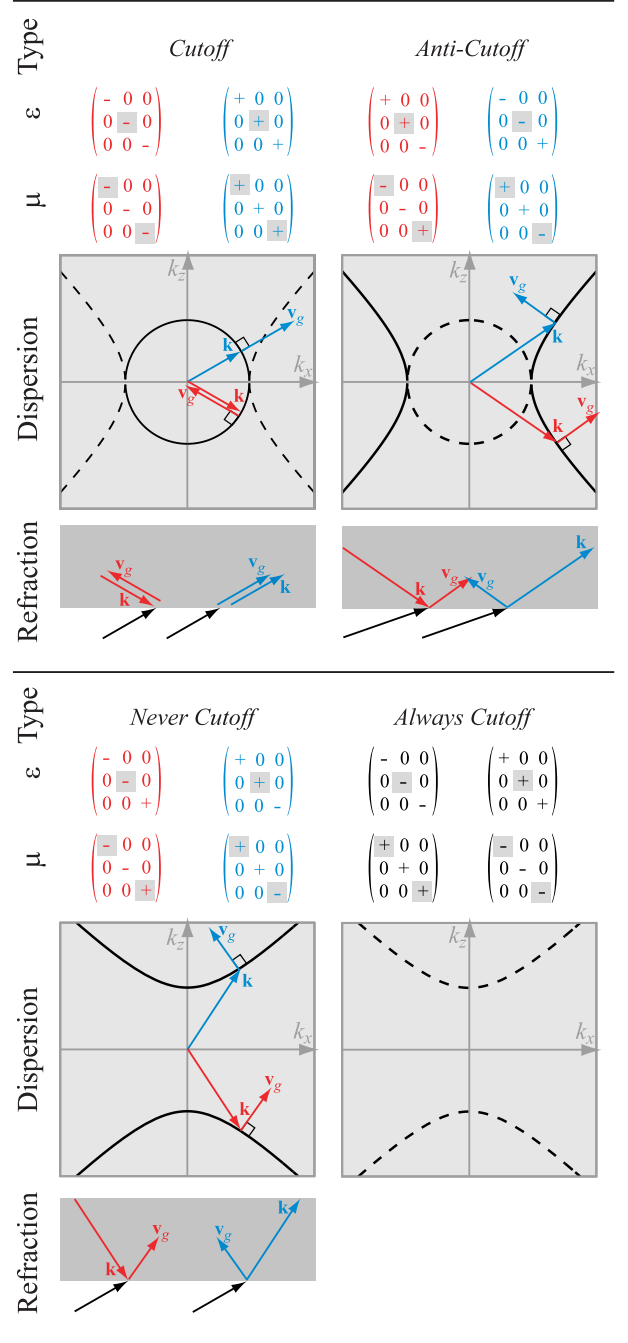


FIG. 2: Material property tensor forms, dispersion plot, and refraction diagram for four classes of media. Each of these media has two sub-types: one positive (blue) and one negative (red) refracting, with the exception that *always cutoff* media does not support propagation and refraction. The dispersion plot shows the relationship between the components of the wave vector at fixed frequency. k_x (horizontal axis) is always real, k_z (vertical axis) can be real (solid line) or imaginary (dashed line). The same wave vector and group velocity vectors are shown in the dispersion plot and the refraction diagram. \mathbf{v}_g shows direction only. The shaded diagonal tensor elements are responsible for the shown behavior for electric y -polarization, the unshaded diagonal elements for magnetic y -polarization.

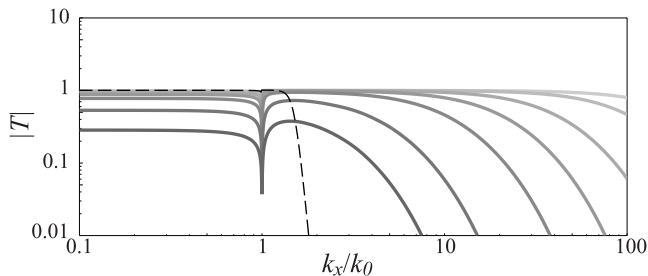


FIG. 3: Magnitude of the transfer function vs. transverse wave vector, k_x , for a bilayer composed of positive and negative refracting *never cutoff* media. Material property elements are of unit magnitude and layers of equal thickness, $L/\lambda = 0.1, 0.2, 0.5, 1, 2$. The thinnest layer is the darkest curve. A realistic loss of $0.01i$ has been added to each diagonal component of ϵ and μ . For comparison, a single layer, isotropic near field lens is shown dashed. The single layer has thickness, λ , and $\epsilon = \mu = -1 + 0.001i$.

layer. If the signs of q_{z1} and q_{z2} are opposite as mentioned above, the phase advances across the two layers can be made equal and opposite, $\phi + \psi = 0$. If we further have the condition that the two layers are impedance matched to each other, $Z_1 = 1$, then Eq. (4), reduces to $T = 1$. In the absence of loss, the material properties can be chosen so that this occurs for all values of the transverse wave vector, k_x . A transfer function with some realistic loss added is shown in Fig 3.

A proposed implementation is shown in Fig. 1. The elements shown in the top and bottom of the figure will implement media that focuses electric y -polarized and magnetic y -polarized waves respectively. Combining the two structures results in a bilayer that focuses both polarizations and is x - y isotropic. The materials are formed from split ring resonators and wires with numerically and experimentally confirmed effective material properties [10]. Each split ring resonator orientation implements negative permeability along a single axis, as does each wire orientation for negative permittivity.

While compensated bilayers of indefinite media exhibit reduced impedance mismatch to free space and high transmission, uncompensated semi-infinite indefinite media exhibit unique high reflection properties. Aside from *cutoff* materials, all other classes of indefinite media have a reflection coefficient amplitude near unity for incident propagating waves. The phase of the reflection coefficient, however, varies, as illustrated here for positive refracting *anti-cutoff* media. The reflection coefficient for electric y -polarization is given by

$$\rho = \frac{\mu_x k_z - q_z}{\mu_x k_z + q_z} \quad (6)$$

where \mathbf{k} and \mathbf{q} are the wave vectors in vacuum and the media respectively. For unit magnitude *anti-cutoff* ma-

terial we have, from Eq. (3),

$$q_z^2 = -\frac{\omega^2}{c^2} + k_x^2 = -k_z^2 \quad (7)$$

Thus $q_z = \pm i k_z$. The correct sign for positive refracting media, $+$, is determined by the requirement that the fields must not diverge in the domain of the solution. We then have

$$\rho = \frac{1 - i}{1 + i} = -i \quad (8)$$

The magnitude of the reflection coefficient is unity, with a phase of -90° for propagating modes of all incident angles. An electric dipole antenna placed $\lambda/8$ away from the surface would thus be enhanced by interaction with this “mirror” surface. Customized reflecting surfaces are of practical interest, as they enhance the efficiency of nearby antennas, while at the same time providing shielding [20, 21]. In this case, the invariance of the reflection phase over all angles of incidence may be advantageous. Furthermore, surface modes, which correspond to poles in Eq. 6, are not supported on this interface. Surface modes require evanescent solutions on both sides of the interface. It is possible, as shown in Fig. 2, to have no overlap of evanescent solutions (dashed line) between *cutoff* and *anti-cutoff* media. In many communications applications the energy lost to the excitation of surface modes is undesirable, as it represents loss of signal.

In conclusion, we have begun to explore the properties of media with indefinite ϵ and μ tensors. Indefinite media are governed by hyperbolic dispersion relations, previously found in more exotic situations, such as relativistic moving media [22]. Consideration of layered structures has led to useful and interesting reflection and refraction behavior, including a new mechanism for sub-diffraction focusing. We note that neither the analysis nor the fabrication of these media is complicated, and thus anticipate other researchers will quickly assimilate the principles and design structures with unique and technologically relevant properties.

We thank Claudio Parazzoli (Phantom Works, Boeing) for motivating this work. This work was supported by DARPA through grants from ONR (Contract No. N00014-00-1-0632) and AFOSR (Contract No. 78535A/416250/440000) and a grant from AFOSR (Contract Number F49620-01-1-0440).

-
- [1] S. John and T. Quang, Phys. Rev. Lett. **74**, 3419+ (1995).
 - [2] A. F. Koenderink *et al.*, Phys. Rev. Lett. **88**, 143903/1 (2002).
 - [3] H. Kosaka *et al.*, Phys. Rev. B **58**, R10096 (1998).
 - [4] M. Notomi, Phys. Rev. B **62**, 10696+ (2000).

- [5] B. Gralak, S. Enoch, and G. Tayeb, *J. Opt. Soc. Am. A* **17**, 1012+ (2000).
- [6] P. Halevi, A. A. Krokhin, and J. Arriaga, *Phys. Rev. Lett.* **82**, 719+ (1999).
- [7] D. R. Smith *et al.*, *Phys. Rev. Lett.* **84**, 4184+ (2000).
- [8] V. G. Veselago, *Sov. Phys. Usp.* **10**, 509+ (1968).
- [9] D. R. Smith and N. Kroll, *Phys. Rev. Lett.* **85**, 3966+ (2000).
- [10] R. A. Shelby, D. R. Smith, and S. Schultz, *Science* **292**, 79+ (2001).
- [11] J. B. Pendry, *Phys. Rev. Lett.* **85**, 3966+ (2000).
- [12] P. M. Valanju, R. M. Walser, and A. P. Valanju, *Phys. Rev. Lett.* **88**, 187401+ (2002).
- [13] N. Garcia and M. Nieto-Vesperinas, *Phys. Rev. Lett.* **88**, 207403 (2002).
- [14] J. A. Kong, B. Wu, and Y. Zhang, *Appl. Phys. Lett.* **80**, 2084+ (2002).
- [15] D. R. Smith, J. B. Pendry, and D. Schurig, in press at *Appl. Phys. Lett.* (unpublished).
- [16] I. V. Lindell, S. A. Tretyakov, K. I. Nikoskinen, and S. Ilvonen, *Microwave and Optical Technology Letters* **31**, 129+ (2001).
- [17] R. Marques, F. Medina, and R. Rafii-El-Idrissi, *Phys. Rev. B* **65**, 144440 (2002).
- [18] L. D. Landau, E. M. Lifshitz, and L. P. Pitaevskii, in *Electrodynamics of Continuous Media* (Pergamon Press, New York, 1984), Chap. X.
- [19] R. W. Ziolkowski and E. Heyman, *Phys. Rev. E* **6405**, 056625+ (2001).
- [20] D. Sievenpiper *et al.*, *IEEE Transactions on Microwave Theory and Techniques* **47**, 2059+ (1999).
- [21] K.-P. Ma, Y. Qian, and T. Itoh, *IEEE Transactions on Microwave Theory and Techniques* **47**, 1509+ (1999).
- [22] J. A. Kong, *Electromagnetic Wave Theory* (Wiley-Interscience, New York, 1990).